Inorg. Chem. **2005**, *44*, 3396–3404

Electropolymerization of Vinylbipyridine Complexes of Ruthenium(II) and Osmium(II) in SiO_2 Sol–Gel Films

John Yang,[†] Milan Sykora,[‡] and Thomas J. Meyer*

Department of Chemistry, University of North Carolina at Chapel Hill, CB# 3290, Chapel Hill, North Carolina 27599-3290, and Los Alamos National Laboratory, C-PCS, MS J567, Los Alamos, New Mexico 87545

Received October 1, 2004

PF_6^- salts of the complexes $[Ru(vbpy)_3]^{2+}$ and $[Os(vbpy)_3]^{2+}$ (vbpy = 4-methyl-4′-vinyl-2,2′-bipyridine) have been electropolymerized into the pores of SiO_2 sol–gel films deposited on conductive Tin(IV)-doped indium oxide-coated glass slides (ITO, In_2O_3:Sn). The resulting transparent composites represent a new class of materials of general formulas ITO/SG-poly-$[Ru(vbpy)_3](PF_6)_2$ and ITO/SG-poly-$[Os(vbpy)_3](PF_6)_2$. The composites are stable with respect to loss of complexes to the external solution and demonstrate several interesting phenomena: (1) Sol–gel pores, serving as diffusion channels for the vbpy complexes and counterions, play a key role in the formation of the polymer and dictate the electrochemical properties of the resulting composite. (2) Dynamic polymer growth occurs within individual diffusion channels creating parallel structures of filled and unfilled channels. (3) Unidirectional charge transfer and a "bilayer" effect have been shown to operate in ITO/SG-poly-$[Ru(vbpy)_3](PF_6)_2$ films exposed to $[Os(vbpy)_3](PF_6)_2$ in the external solution. (4) Photophysical properties of the metal-to-ligand charge transfer (MLCT) excited states in ITO/SG-poly-$[Ru(vbpy)_3](PF_6)_2$ composites are significantly modified compared to electropolymerized films on ITO or model monomeric complexes in solution.

Transparent SiO_2 sol−gels are inexpensive and simple to manufacture while retaining the high durability of glasses and the porosity of ceramics.[1−5] The low-temperature manufacturing process allows for the sol−gels to be used as molecular hosts by exchange and immobilization. The introduction of molecular species within sol−gel materials has led to the development of new classes of composite materials for applications in optical devices,[6−9] chemical and biomolecular sensors,[10−14] and catalysis.[15] A number of these applications have demonstrated commercial potential.

The search for optical devices or sensors utilizing luminescence of a well-studied chromophore has given rise to a number of reports of immobilization of ruthenium(II) polypyridyl complexes in solid gels.[16−23] The environmental

* Author to whom correspondence should be addressed. E-mail: tjmeyer@lanl.gov.
[†] University of North Carolina at Chapel Hill.
[‡] Los Alamos National Laboratory, C-PCS.

(1) Brinker, C. J.; Clark, B. E.; Ulrich, D. R., Eds. *Better Ceramics Through Chemistry II*; Materials Research Society: Pittsburgh, PA, 1986; Vol. 73.
(2) Brinker, C. J. *J. Non-Cryst. Solids* **1988**, *100*, 31−50.
(3) Brinker, C. J.; Scherer, G. W. *Sol−Gel Science: The Physics and Chemistry of Sol−Gel Processing*; Academic Press: Boston, MA, 1990.
(4) Hench, L. L., Ulrich, D. R., Eds. *Science of Ceramic Chemical Processing*; J. Wiley: New York, 1986.
(5) Hench, L. L.; West, J. K. *Chem. Rev.* **1990**, *90*, 33−72.
(6) Dunn, B.; Zink, J. I. *J. Mater. Chem.* **1991**, *1*, 903−913.
(7) Klein, L. C., Ed. *Sol−Gel Optics: Processing and Applications*; Kluwer Academic Publishers: Boston, MA, 1994.
(8) Avnir, D. *Acc. Chem. Res.* **1995**, *28*, 328−334.
(9) Levy, D. *Chem. Mater.* **1997**, *9*, 2666−2670.
(10) Lev, O.; Tsionsky, M.; Rabinovich, L.; Glezer, V.; Sampath, S.; Pankratov, I.; Gun, J. *Anal. Chem.* **1995**, *67*, 22A−30A.
(11) Collinson, M. M.; Howells, A. R. *Anal. Chem.* **2000**, *72*, 702A−709A.
(12) Lin, J.; Brown, C. W. *Trends Anal. Chem.* **1997**, *16*, 200−211.
(13) Livage, J.; Coradin, T.; Roux, C. *J. Phys: Condens. Matter* **2001**, *13*, R673−691.
(14) Jin, W.; Brennan, J. D. *Anal. Chim. Acta* **2002**, *461*, 1−36.
(15) Lu, Z. L.; Lindner, E.; Mayer, H. A. *Chem. Rev.* **2002**, *102*, 3543−3577.
(16) Avnir, D.; Kaufman, V. R.; Reisfeld, R. *J. Non-Cryst. Solids* **1985**, *74*, 395−406.
(17) Matsui, K.; Sasaki, K.; Takahashi, N. *Langmuir* **1991**, *7*, 2866.
(18) Dvorak, O.; DeArmond, K. M. *J. Phys. Chem.* **1993**, *97*, 2646−2648.
(19) Castellano, F. N.; Heimer, T. A.; Tandhasetti, M. T.; Meyer, G. J. *Chem. Mater.* **1994**, *6*, 1041.
(20) Castellano, F. N.; Meyer, G. J. In *Molecular Level Artificial Photosynthetic Materials*; Meyer, G. J., Ed.; John Wiley & Sons: New York, 1997; Vol. 44, pp 167−208.
(21) Innocenzi, P.; Kozuka, H.; Yoko, T. *J. Phys. Chem. B* **1997**, *101*, 2285−2291.
(22) Sykora, M.; Meyer, T. J. *Chem. Mater.* **1999**, *11*, 1186−1189.

10.1021/ic048623r CCC: $30.25 © 2005 American Chemical Society
Published on Web 04/12/2005

heterogeneity of these systems at the microscopic level typically makes characterization of photophysical properties of entrapped ions complicated,[19−21] but interest in this area has grown owing to the unique ground- and excited-state properties of Ru(II) polypyridyl complexes.

With the sol−gels exposed to solution a major problem exists with most doped and ion-exchanged materials arising from leaching of dopants into the external solution. In the case of Ru(II) polypyridyl complexes the strategies that have been shown to be effective in overcoming this problem utilize polymers[22,24] (i.e., molecules larger than sol−gel pore size) or covalent attachment of the complex directly to the SiO_2 framework.[25,26] Incorporation of macromolecules is a general procedure since the macromolecule is incorporated into the sol prior to gelation. Covalently attaching molecules to the inner matrix of the sol−gel requires synthetic modification of the dopant and can lead to a significant alteration in the gelation process and dopant properties.

In this manuscript we describe an alternate approach to preparing stable sol−gel composites of Ru(II) and Os(II) polypyridyl complexes. It is based on the reductive electropolymerization of Ru(II)− and Os(II)−vinylbipyridyl derivatives within the pores of SiO_2 sol−gel films. It is similar to the approach used in the preparation of polyaniline sol−gel composites reported previously.[27] In the resulting sol−gel composites we have been able to demonstrate the existence of a series of interesting phenomena:

(1) the importance of diffusion channels and their role in forming polymers, restricting diffusion and creating parallel structures in which there are filled and unfilled channels;

(2) a "bilayer" effect with directional charge-transfer involving an external Os^{II} couple;

(3) significantly modified photophysical properties of metal-to-ligand charge transfer (MLCT) excited states compared to related excited states in electropolymerized films or in solution.

Experimental Section

Materials and Synthesis. The solvents acetonitrile (CH_3CN: Baxter; Burdick & Jackson, high purity), ethyl acetate (EtOAc: Fisher), toluene (Fisher), and ethanol (EtOH: AAPER Alcohol and Chemical Co, absolute) were used as received. Tetramethyl orthosilicate ($Si(OCH_3)_4$, TMOS), poly(ethylene glycol) (PEG-2000), ammonium hexafluorophosphate (NH_4PF_6), and Triton X-100 (TX100) were obtained from Aldrich and used as received. Tin(IV)-doped indium oxide-coated glass slides (ITO, In_2O_3:Sn; Delta Technologies, Ltd.) were soniccated in EtOH and H_2O and dried before use.

4-Methyl-4′-vinyl-2,2′-bipyridine (vbpy) was prepared according to a literature procedure[28] and purified prior to use by column chromatography on alumina with a 1:4 EtOAc/hexanes eluent. $[Ru(vbpy)_3](PF_6)_2$ and $[Ru(dmb)_3](PF_6)_2$ were synthesized according to procedures reported previously.[29,30]

$[Os(vbpy)_3](PF_6)_2$ was synthesized by using a one-pot method. Briefly, to a 50 mL round-bottom flask were added 260 mg of $(NH_4)OsCl_6$ (Johnson Mathey), 360 mg of vbpy, 12 mL of ethylene glycol (Fisher), and 270 mg of hydroquinone (Mallinckrodt). The mixture was heated at reflux under argon for 3 h and allowed to cool, at which time a concentrated aqueous solution of NH_4PF_6 (∼3 mL) was added to form a hard to stir brownish-green slurry. After being filtered and rinsed with a small amount of cold water, the slurry was dissolved in a minimal amount of CH_3CN and dropped into rapidly stirring ether. Large, dark green crystals were collected at this point (>80% yield). Before use this salt was purified by alumina chromatography with a 1:1 CH_3CN/toluene eluent. The desired salt was collected as a primary, dark green band which was the second component eluted.

Sol−Gel Preparation. The sol−gel was prepared through the acid-catalyzed metal alkoxide hydrolysis and condensation process summarized below.[2,3]

hydrolysis:

$$Si(OMe)_4 + H_2O \rightarrow HO-Si(OMe)_3 + MeOH$$

condensation:

$$\equiv Si-OMe + \equiv Si-OH \rightarrow \equiv Si-O-Si\equiv + MeOH$$

$$\equiv Si-OH + \equiv Si-OH \rightarrow \equiv Si-O-Si\equiv + HOH$$

A procedure described previously was followed.[22,24] Briefly, to 0.85 mL of continuously stirred absolute EtOH were added 10−15 drops (∼0.15 g) of surface active agent TX100, 0.1 mL of 0.01 M $HClO_4$, and 0.2 mL of TMOS. The mixture was stirred for 15 min between each addition and aged for 24 h. Thin (∼100 nm) sol−gel film samples were prepared by spin-coating the aged mixture onto an ITO electrode at 5000 rpm. After being allowed to dry at room temperature (∼ 1 h), the films were allowed to age for an additional 24 h at 100 °C. The sol−gel films on ITO (SG/ITO) were used within 3 days to ensure similar aging among different batches of sol−gel samples.

Electropolymerization. Reductive electropolymerization of Ru(II) and Os(II) vinylbipyridine-containing complexes within sol−gel films was accomplished by using procedures first described by Murray and Meyer et al.[31,32] Reduction was conducted in a two-compartment cell separated by a frit. One compartment contained ∼1 mM $[Ru(vbpy)_3]^{2+}$ in acetonitrile (with 0.1 M TBAH supporting electrolyte), the working sol−gel on ITO (SG/ITO) electrode, and the Pt mesh auxiliary electrode. The other compartment contained the reference electrode (Ag wire/$AgNO_3$ at 0.01 M, +300 mV vs SCE) in 0.1 M TBAH/CH_3CN. This configuration was used to prevent the reference electrode from being clogged with the metal complex. The working electrode was either scanned reductively or the potential was held past the reduction potential for reduction of the coordinated vinylbipyridine ligands. Better reproducibility was obtained by using the scanning method. Typically, the potentiostat

(23) Collinson, M. M.; Novak, B.; Martin, S. A.; Taussig, J. S. *Anal. Chem.* **2000**, *72*, 2914−2918.
(24) Sykora, M.; Maxwell, K. A.; Meyer, T. J. *Inorg. Chem.* **1999**, *38*, 3596−3597.
(25) Malins, C.; Fanni, S.; Glever, H. G.; Vos, J. G.; MacCraith, B. D. *Anal. Commun.* **1999**, *36*, 3−4.
(26) Lee, J. K.; Lee, S. H.; Kim, M.; Kim, H.; Kim, D. H.; Lee, W. Y. *Chem. Commun.* **2003**, 1602−1603.
(27) Verghese, M. M.; Ramanathan, K.; Ashraf, S. M.; Kamalasanan, M. N.; Malhotra, B. D. *Chem. Mater.* **1996**, *8*, 822−824.
(28) Leasure, R. M.; Ou, W.; Moss, J. A.; Linton, R. W.; Meyer, T. J. *Chem. Mater.* **1996**, *8*, 264−273.
(29) Abruna, H. D.; Denisevich, P.; Umana, M.; Meyer, T. J. *J. Am. Chem. Soc.* **1981**, *103*, 1.
(30) Treadway, J. A. Ph.D. Thesis, University of North Carolina, Chapel Hill, NC, 1998.
(31) Calvert, J. M.; Schmehl, R. H.; Sullivan, B. P.; Facci, J. S.; Meyer, T. J.; Murray, R. W. *Inorg. Chem.* **1983**, *22*, 2151−2162.
(32) Denisevich, P.; Abruna, H. D.; Leidner, C. R.; Meyer, T. J.; Murray, R. W. *Inorg. Chem.* **1982**, *21*, 2153−2161.

(Princeton Applied Research 270, EG&G) was scanned negatively in multiple sweeps past the first and second vinylbipyridine ligand reductions (to −2.0 V vs $Ag/AgNO_3$ at 100 mV/s).

In later experiments, the effect of scans to negative potential on the diffusional characteristics of the films was recognized. This is discussed in detail in a later section of this article. This led to a modification of the electropolymerization procedure and the use of fewer negative scans and solutions more concentrated in $[Ru(vbpy)_3]^{2+}$ (up to 5 mM).

Film Characterization. The growth of sol−gel electropolymerized films was monitored by UV−visible and cyclic voltammetric measurements. Increases in absorption at the $Ru^{II} \rightarrow$ vbpy metal-to-ligand charge transfer (MLCT) maximum at 460 nm were monitored with a HP-8452 dide array spectrometer through successive electropolymerization cycles. Measurements were conducted either with the electrode immersed in acetonitrile in a spectrophotometric cell or as a dry film in the path of the monitoring beam. The two methods yielded similar results after absorption from a blank electrode was subtracted from the sample measurements.

The number of moles of metal complex/cm^2 of projected surface area of the nanocrystalline film, effective surface coverage, Γ_{eff} (mol/cm^2), was calculated from the relationship $\Gamma_{eff} = A(\lambda)/\sigma(\lambda)$. $A(\lambda)$ is the absorbance of the film, and $\sigma(\lambda)$ is the absorption cross section in units of cm^2/mol obtained from the decadic molar extinction coefficient ϵ (M^{-1} cm^{-1}) by multiplication by 1000 cm^3/L. In the analyses, ϵ(458 nm) = 13 000 M^{-1} cm^{-1} was used for electropolymerized $[Ru(vbpy)_3]^{2+}$.

Cyclic voltammograms of electropolymerized films on SG/ITO were measured in 0.1 M TBAH/CH_3CN with an $Ag/AgNO_3$ reference (+0.300 V vs SCE), and all potentials hereafter are reported versus $Ag/AgNO_3$. The potentiostat was scanned at 100 mV/s from 0 to 1.5 V to examine the $Ru^{III/II}$ couple in the electropolymerized film, which occurred at $E_{1/2}$ = 0.95 V. These measurements were conducted prior to photophysical measurements since immersion of the film washed out any unpolymerized $[Ru(vbpy)_3]^{2+}$.

The photophysical properties of the electropolymerized films were characterized by steady state emission and lifetime measurements. Steady state emission spectra were recorded at room temperature on a Spex Fluorolog-F212 emission spectrometer equipped with a 450-W xenon lamp and a cooled R928 photomultiplier tube. The films were individually placed in a sealable modified fluorescence cuvette, which allowed for deaeration with argon prior to measurement. A Teflon spacer at the bottom of the cuvette was used to support the film to minimize movement and variations in sampling positions. The samples were excited at a 45° angle facing the excitation beam, and the emission was collected at an angle of 90° to the excitation source. The spectra were corrected for detector wavelength response by using correction factors supplied by the manufacturer.

Excited-state lifetimes were measured in the same cuvette with laser flash excitation at 455 nm by using a PRA nitrogen laser (model LN1000) pumping a PRA dye laser (model LN102). The decay of Ru^{II*} MLCT emission was monitored at 640 nm by using a PRA monochromator (model B204-3) and a Hamamatsu R-928 photo multiplier tube. For emission measurements on electropolymerized samples the monochromator entrance and exit slits were opened wide (4 mm) to capture the weak emission. The signal was recorded on a LeCroy 7200A digital oscilloscope interfaced to a PC by using LabView software. The excited-state lifetimes were determined by fitting the experimental data to a multiexponential expression (eq 1), and weighted averaged lifetimes were calculated by using eq 2.

One to three components were used in the analyses depending on the complexity of the decays.

$$I = I_0 + \sum_{i=1}^{3} I_i \exp(-t/\tau_i) \quad (1)$$

$$\langle\tau\rangle = \sum_{i=1}^{3} I_i\tau_i / \sum_{i=1}^{3} I_i \quad (2)$$

Film depth profiles were obtained by X-ray photoelectron spectroscopy (XPS) on a Perkin-Elmer Physical Electronics model 5400 spectrometer. A differentially pumped Ar^+ ion gun (4 kV, 25 mA emission current) was used to sputter the film surface, and a Mg Kα X-ray source (400 W, 15 kV) to irradiate the exposed surface over 2-min sputter intervals. The sputtered area was approximately 10 mm^2, and the analyzed area 0.95 mm^2. The hemispherical analyzer pass energy was 35.75 eV, and the angle of collection 45°. Quantitative atomic ratios were calculated by using instrumental sensitivity factors and integrated photoelectron peak areas.

Results

Formation and Characterization of Sol−Gel Electropolymerized Poly-$[Ru(vbpy)_3](PF_6)_2$. In cyclic voltammograms of the $Ru^{III/II}$ couple for $Ru(vbpy)_3^{2+}$ at ITO and ITO/SG electrode there is a shift in $E_{1/2}$ from 870 mV at ITO to 850 mV at ITO/SG and an increase in peak-to-peak separation ($\Delta E_p = E_{p,a} - E_{p,c}$ with E_p the anodic and cathodic peak potentials) from 90 to 160 mV at a scan rate of 100 mV/s. The kinetic inhibition at ITO/SG suggested by the increase in ΔE_p is a consequence of sluggish diffusion through the narrow channels and pores.[24]

Electropolymerization of $[Ru(vbpy)_3](PF_6)_2$ at ITO/SG is illustrated in Figure 1A and compared with electropolymerization at a bare ITO electrode in Figure 1B. Similar growths in current with increasing number of scans are observed in both experiments. However, there is a significant shift to more negative peak potentials with each scan at ITO/SG. This may be due to the restrictive nature of the sol−gel matrix toward diffusion, which hinders electrolyte mobility. As electropolymerized film is deposited within the pores of the sol−gel, diffusion is further inhibited and this diffusion-limitation results in less reversible CV's.[33,34]

As shown by oxidative scans following electropolymerization, reductive electropolymerization results in a growth in current for the $Ru^{III/II}$ couple. The $Ru^{III/II}$ wave after five electropolymerization scans is shown in Figure 2. This growth is not due to simple ion exchange. Blank experiments

(33) The decreased CV reversibility can be also partially due to side processes involving reduced $[Ru(vbpy)_3](PF_6)_2$ and the sol−gel or sol−gel components such as trace water and/or EtOH remaining in the sol−gel pores after sol−gel preparation and drying. The extent and nature of potential side reactions have not been investigated.

(34) Because the asymmetry of vbpy ligands the synthesis of $[Ru(vbpy)_3](PF_6)_2$ yields a mixture of positional isomers, copolymerization of these isomers introduces an additional element of heterogeneity into the resulting composite. The photophysical properties of separated positional isomers of a related Ru^{II} complex have been studied previously (Treadway, J. A.; Chen, P. Y.; Rutherford, T. J.; Keene, R. F.; Meyer T. J. *J. Phys. Chem. A* **1997**, *101*, 6824−6826). In the present work no attempt was made to separate the isomers prior to electropolymerization.

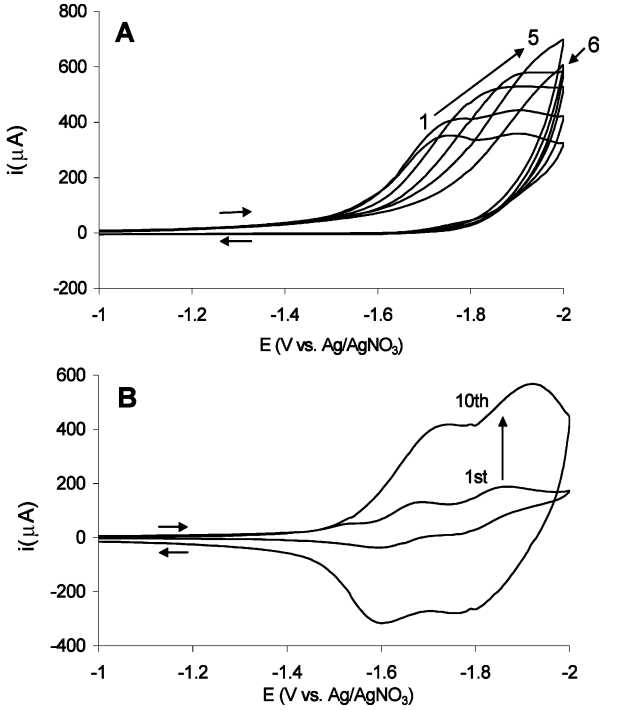

Figure 1. Cyclic voltammograms showing reductive scans at 100 mV/s from 0 V → −2.0 V → 0 V in a 3 mM solution of $Ru(vbpy)_3^{2+}$ in acetonitrile, 0.1 M in TBAH: (A) for an ITO/SG electrode scanning reductively, first six scans shown; (B) for a bare ITO electrode scanning reductively, 1st and 10th cycles shown.

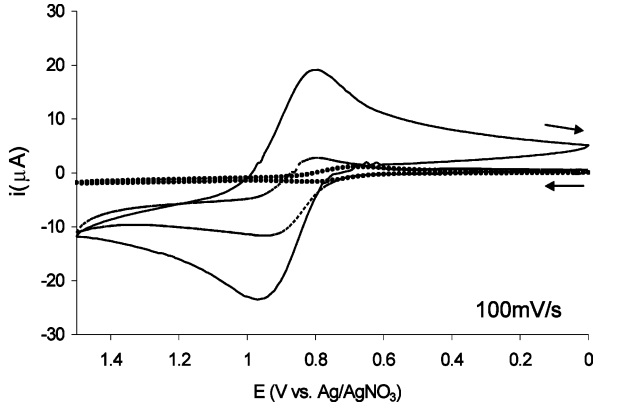

Figure 2. Oxidative cyclic voltammograms of ITO/SG-Ru composites in fresh CH_3CN (0.1 M in TBAH) prepared by three different methods: solid line, ITO/SG-poly-$[Ru(vbpy)_3](PF_6)_2$ prepared by 5 reductive electropolymerization sweeps (conditions as in Figure 1); dashed line, ITO/SG-$[Ru(vbpy)_3]^{2+}$ prepared by ion-exchange by exposing an ITO/SG film to a 3 mM solution of $[Ru(vbpy)_3]^{2+}$ in acetonitrile overnight; dotted line, ITO/SG-$[Ru(dmb)_3](PF_6)_2$ prepared by 5 reductive electropolymerization sweeps in a 3 mM solution of nonpolymerizable $[Ru(dmb)_3]^{2+}$ in acetonitrile (conditions as in Figure 1).

with $[Ru(dmb)_3]^{2+}$ (dmb is 4,4′-dimethyl-2,2′-bipyridine) showed that when an electrode exposed to $[Ru(dmb)_3]^{2+}$ was subjected to the same electropolymerization treatment, the initial electroactivity of the $Ru^{III/II}$ couple was lost after several oxidative scans in fresh acetonitrile due to diffusion of the complex out of the sol−gel (Figure 2). Growth of the electropolymerized film in SG/ITO monitored by UV−visible measurements is shown in Figure 3.

The growth of poly-$[Ru(vbpy)_3](PF_6)_2$ within the sol−gel was examined by XPS spectroscopy with depth profiling.

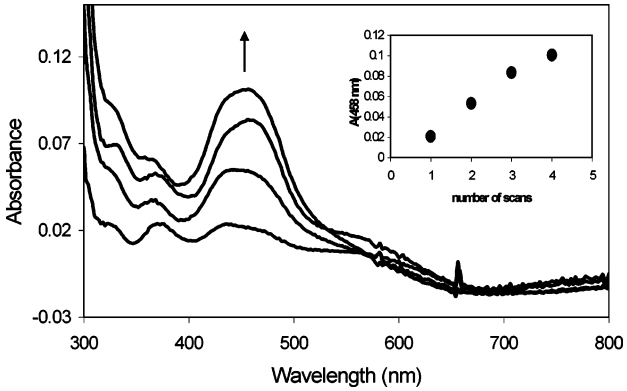

Figure 3. Absorption spectra at an ITO/SG-poly-$[Ru(vbpy)_3](PF_6)_2$ electrode as a function of the number of reductive electropolymerization scans. The inset shows the increase at $\lambda = 458$ nm as a function of the number of scans. Conditions are as in Figure 1.

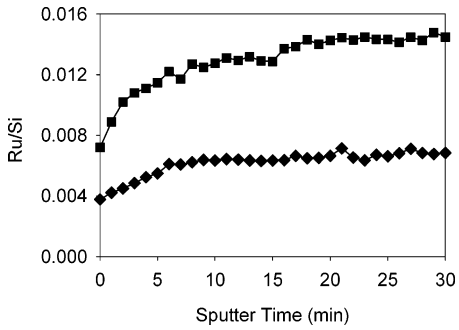

Figure 4. Depth profile for the surface of an ITO/SG-poly-$[Ru(vbpy)_3]$-$(PF_6)_2$ electrode prepared as in Figure 1 after 1 (◆) and 15 (■) reductive scans (to −1.6 V) showing the change in Ru/Si ratio as a function of sputter time (depth).

In Figure 4 are shown plots of the Ru/Si atom ratio as a function of sputter time which provides information about Ru content from the solution−film interface into the bulk of the film. Comparison of Ru/Si ratios for ion-exchanged compared to electropolymerized $[Ru(vbpy)_3]^{2+}$ showed that electropolymerization increases the Ru/Si ratio by factors of 5−10. As shown in Figure 4, the Ru/Si ratio increases with the number of electropolymerization scans as expected. There is a distribution in Ru content with Ru increasing from the external film interface into the bulk where Ru/Si ∼ 0.015 is reached and a ratio of ∼1 complex site/50 Si atoms. Comparable and even higher loadings up to Ru/Si ∼ 0.1 can be obtained by adding $[Ru(bpy)_3]Cl_2$ to the reacting sol−gel medium as it forms. However, under these conditions only parts of the metal complex sites are electroactive and $[Ru(bpy)_3]^{2+}$ is lost to an external solution over time.[35]

Photophysical Properties. Steady state emission and lifetime data for the MLCT excited states of poly-$[Ru(vbpy)_3]$-$(PF_6)_2$ electropolymerized on ITO or in ITO/SG are shown in Figure 5A and summarized in Table 1. The emission maxima at 652 nm in ITO/SG and especially at 680 nm on ITO are significantly red-shifted compared to $\lambda_{max} = 642$ for the model complex $[Ru(dmb)_3]^{2+}$ in CH_3CN. The emission decays display distinctive fast relaxation processes in both poly-$[Ru(vbpy)_3](PF_6)_2$ electropolymerized in

(35) Sykora, M.; Meyer, T. J. Unpublished results.

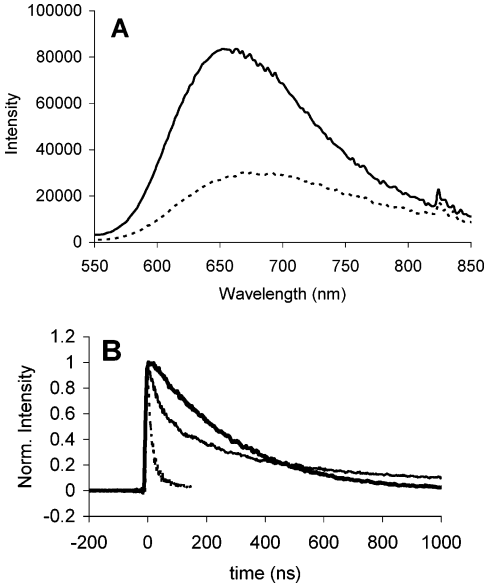

Figure 5. (A) Steady-state emission spectra for ITO/poly-$[Ru(vbpy)_3](PF_6)_2$ ($\Gamma = 2.2 \times 10^{-8}$ M cm^{-2}; see text) (dashed line) and ITO/SG-poly-$[Ru(vbpy)_3](PF_6)_2$ ($\Gamma \sim 1 \times 10^{-8}$ M cm^{-2}) (solid line) electrodes prepared as in Figure 1. Both samples were measured as dry films under a N_2 atmosphere. (B) Excited-state lifetime decay traces comparing ITO/poly-$[Ru(vbpy)_3](PF_6)_2$ (dashed line) and ITO/SG-poly-$[Ru(vbpy)_3](PF_6)_2$ (solid line) films following 10 reductive electropolymerization sweeps under conditions as in Figure 1. Both samples were measured as dry films under N_2 atmospheres. The luminescence decay of $Ru(vbpy)_3^{2+*}$ in deaerated acetonitrile solution (thick solid line) is also shown for comparison.

ITO/SG and on ITO. The rapid relaxation kinetics of ITO-poly-$[Ru(vbpy)_3](PF_6)_2$ have been observed and studied previously.[36]

In a relative sense, emission from Ru^{II*} in SG/ITO is more efficient than in films electropolymerized directly on bare ITO. This is illustrated by the data in Figure 5A and the relative emission intensities of samples measured on the same day. The spectrum of ITO/poly-$[Ru(vbpy)_3](PF_6)_2$ was obtained following 10 electropolymerization cycles giving an effective surface coverage of $\Gamma = 2.2 \times 10^{-8}$ M cm^{-2}. The spectrum in ITO/SG-poly-$[Ru(vbpy)_3](PF_6)_2$ was obtained by following 20 reductive electropolymerization cycles which gave a coverage of $\Gamma \sim 1 \times 10^{-8}$ M cm^{-2}. After correction for different absorptivities at the excitation wavelength, the comparison of relative emission intensities reveals that the intensity/Ru^{II} is $\sim$ 10 times greater in ITO/SG.

Bilayer Effects. Attempts to prepare spatially controlled, well-defined bilayers of ITO/SG-poly-$[Ru(vbpy)_3](PF_6)_2$,-poly-$[Os(vbpy)_3](PF_6)_2$ were unsuccessful. Repeated attempts to form bilayers were made by first electropolymerizing controlled amounts of $[Ru(vbpy)_3]^{2+}$ into ITO/SG followed by electropolymerization of $[Os(vbpy)_3]^{2+}$. With relatively low loadings of poly-$[Ru(vbpy)_3](PF_6)_2$, poly-$[Os(vbpy)_3](PF_6)_2$ forms on the surface through unfilled diffusion channels making direct contact with the ITO electrode when electropolymerization is initiated (see below). A true bilayer effect was not observed.[29,37,38] Rather, reversible redox waves for both $Ru^{III/II}$ and $Os^{III/II}$ couples were observed, showing that direct contact exists between electropolymerized Os^{II} and the electrode surface. For more heavily loaded films, in which the diffusion channels were filled, the electrochemical behavior was ill-defined because occupation of the diffusion channels by the polymer inhibits counterion transport.

Use of ITO/SG/poly-$[Ru(vbpy)_3](PF_6)_2$ composites as redox membranes was investigated with $[Os(vbpy)_3]^{2+}$ in the external solution. The electrode response was found to be sensitive to the extent of loading of the sol−gel film and the scan rate. In Figure 6A is shown a cyclic voltammogram of partly loaded ITO/SG-poly-$[Ru(vbpy)_3](PF_6)_2$ (2 reductive cycles) exposed to an external solution containing $[Os(vbpy)_3]^{2+}$. The presence of a well-defined $Os^{III/II}$ wave near $E_{1/2} = 0.45$ V suggests that the diffusional channel structure within the sol−gel is sufficiently open to allow diffusional access of Os^{II} to the electrode surface. The slight difference in current for the forward and return waves is attributed to a small contribution from charge mediation effects as observed in these materials previously.[24]

The electrode response at a more completely loaded film is shown in Figure 6B. In this case there is no evidence for an $Os^{III/II}$ diffusional wave. An oxidative scan past the Ru(II) → Ru(III) wave reveals a catalytic response (note the significant increase in current) with oxidative peak potential $E_{p,a} = 1.1$ V and a lower reductive current on the reverse scan that varies with the concentration of Os^{II} in external solution. (The shift in catalytic Ru^{II} peak potential and skewing of the wave are characteristics of highly loaded films and are due to slow counterion transport as noted above.) This is consistent with redox bilayer behavior with indirect oxidation of Os^{II} to Os^{III} through the intervening SG-poly-$[Ru(vbpy)_3](PF_6)_2$ film acting as a redox membrane, with indirect oxidation of Os^{II} to Os^{III} following oxidation of Ru^{II} to Ru^{III} in the film. The current for $Os^{III} \rightarrow Os^{II}$ reduction is lower and shifted positively because of slow reduction due to indirect $Ru^{II} \rightarrow Os^{III}$ electron-transfer reduction of Os^{III}; see below.

At the slow scan rate of 5 mV/s, Figure 6C, the voltammetric response takes on the character of a stirred solution voltammogram with diffusion to the film−solution interface adequate to maintain a sustained catalytic current for oxidation of Os^{II} to Os^{III}. Under these conditions, oxidation of Os^{II} to Os^{III} occurs at an apparent $E_{1/2}$ value near the $Ru^{III/II}$ potential. There is a decrease in limiting current on the reverse scan, but the reduction occurs near $E_{1/2}$ for the $Ru^{III/II}$ couple. At this low scan rate, indirect reduction of Os^{III} by initial $Ru^{II} \rightarrow Os^{III}$ electron transfer is sufficiently rapid that the wave shape is only slightly distorted. An additional, smaller wave appears at $E_{1/2} \sim 0.45$ V near the potential for the $Os^{III/II}$ couple.

Sol−Gel Matrix Collapse. Given the negative potentials used in the electropolymerization experiments, we investigated the effect of applied potentials to −2 V on the properties of the sol−gel. This is a legitimate concern since

(36) Devenney, M.; Worl, L. A.; Gould, S.; Guadalupe, A.; Sullivan, B. P.; Caspar, J. P.; Leasure, R. L.; Gardner, J. R.; Meyer, T. J. *J. Phys. Chem. A* **1997**, *101*, 4535−4540.

(37) Denisevich, P.; Willman, K. W.; Murray, R. W. *J. Am. Chem. Soc.* **1981**, *103*, 4727.

(38) Pickup, P. G.; Kutner, W.; Leidner, C. R.; Murray, R. W. *J. Am. Chem. Soc.* **1984**, *106*, 1991−1998.

Table 1. Photophysical Properties of ITO/SG-poly-[Ru(vbpy)$_3$](PF$_6$)$_2$, ITO/poly-[Ru(vbpy)$_3$](PF$_6$)$_2$, and the Model Complex [Ru(dmb)$_3$]$^{2+}$

Material	λ^{abs}_{max} (nm)	λ^{emi}_{max} (nm)	$\tau_1(I_1)^c$ (ns) (%)	$\tau_2(I_2)^c$ (ns) (%)	$\tau_3(I_3)^c$ (ns) (%)	$\langle\tau\rangle^d$ (ns)
ITO/SG-poly-[Ru(vbpy)$_3$] (PF$_6$)$_2$[a]	458	650	4.5 (3)	243 (47)	1074 (50)	646
ITO/poly-[Ru(vbpy)$_3$](PF$_6$)$_2$[a]	458	680	3.3 (86)	37 (14)		8
Ru(dmb)$_3^{2+}$ [b,e]	458	642			950 (100)	950

[a] Dry film under N_2 atmosphere. [b] In deaerated CH_3CN. [c] Excited-state liefetime components and their relative contribution as determined by fitting to eq 1. [d] Average excited-state lifetime calculated by using eq 2. [e] From ref 49.

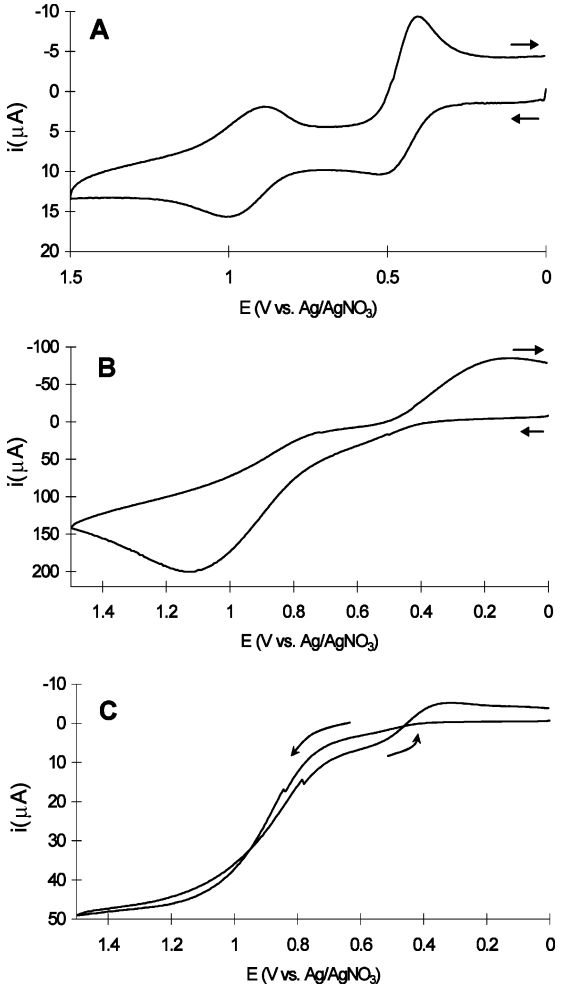

Figure 6. Cyclic voltammograms for (A) ITO/SG-poly-[Ru(vbpy)$_3$](PF$_6$)$_2$ formed by 2 reductive electropolymerization scans under conditions as in Figure 1, scanning oxidatively at 100 mV/s from 0 V → +1.5 V → 0 V in solution 3 mM in Os(vbpy)$_3^{2+}$ in acetonitrile 0.1 M in TBAH, (B) as in (A) except that ITO/SG-poly-[Ru(vbpy)$_3$](PF$_6$)$_2$ was formed by 10 reductive electropolymerization scans, and (C) as in B but at 5 mV/s scan rate.

the pores and channels of the gel matrix have distinct local pH and charge characteristics[39] and scanning to negative potentials may disrupt the local internal structure leading to changes in properties.

In Figure 7 are shown cyclic voltammograms of four electrodes which had been prescanned to −1.1, −1.3, −1.6, or −1.9 V with 20 subsequent sweeps in acetonitrile. Cyclic voltammograms were then recorded in fresh solutions 3 mM in [Os(vbpy)$_3$]$^{2+}$. The impact of negative scanning is apparent in these data. Well-defined Os$^{III/II}$ waves are observed with prescans to −1.1 and −1.3 V, but the electrode response upon scanning to −1.6 or −1.9 V is poorly defined.

(39) Dunn, B.; Zink, J. I. *Chem. Mater.* **1997**, *9*, 2280−2291.

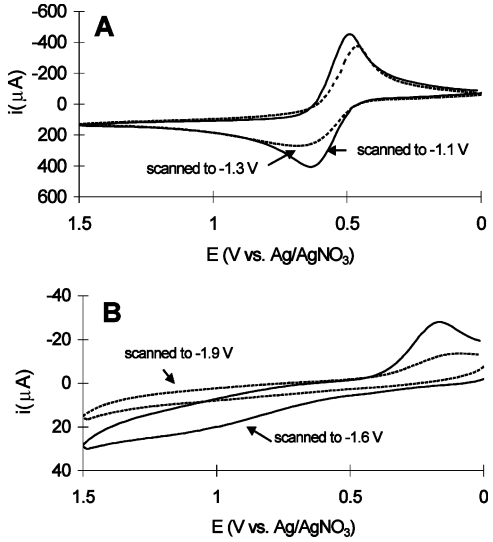

Figure 7. (A, B) Cyclic voltammograms at ITO/SG electrodes (following 20 reductive scans in CH_3CN (0.1 M in TBAH) from 0 V to potentials listed for each CV) at 100 mV/s and then from 0 V → +1.5 V → 0 V in acetonitrile solution 3 mM in [Os(vbpy)$_3$]$^{2+}$.

With this behavior recognized, the electropolymerization procedure was modified with fewer scans and higher concentrations of complex used. Under our conditions fewer than five reductive scans in solutions 3 mM in complex were sufficient to create nearly completely filled ITO/SG films (Figure 3).

Discussion

Reductive electropolymerization of vinylbipyridyl complexes has been achieved on a variety of conducting surfaces.[29] The electropolymerization of [Ru(vbpy)$_3$]$^{2+}$ within the porous microstructure of sol−gel films provides a novel alternative to the overall strategy of immobilization by electropolymerization.

There is a propensity for sol−gel-immobilized species (ion-exchanged, electroexchanged, and predoped) to leach out of conventional sol−gels when exposed to solvents such as acetonitrile or water. Due to the extended, cross-linked nature of an electropolymerized film of complexes, we anticipated that electropolymerization should provide a viable strategy for stabilizing sol−gel materials toward loss of added molecules.

The evidence provided here demonstrates that reductive electropolymerization of [Ru(vbpy)$_3$]$^{2+}$ can occur within the open porous structure of SiO_2 thin films on ITO electrodes. In summary:

(1) Peak currents for the Ru$^{III/II}$ wave increase with the number of reductive scans.

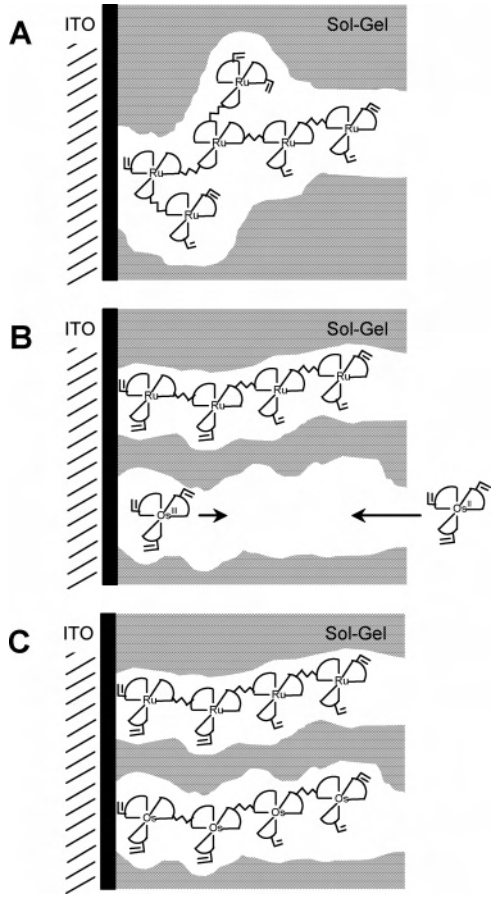

Figure 8. (A) Illustration of the results of reductive electropolymerization of $[Ru(vbpy)_3]^{2+}$ in ITO/SG. (B) Illustration of the sequential electropolymerization of $[Ru(vbpy)_3]^{2+}$ followed by diffusional oxidation of $[Os(vbpy)_3]^{2+}$. (C) Illustration of the proposed resulting parallel channel structure formed upon sequential electropolymerization of $[Ru(vbpy)_3]^{2+}$ and $[Os(vbpy)_3]^{2+}$.

(2) The increase in peak currents is paralleled by an increase in $Ru^{II} \rightarrow$ vbpy MLCT absorption intensity at 458 nm (Figure 3) and an increase in Ru content as shown by XPS (Figure 4).

(3) The resulting composites are completely stable toward loss of complex and contain Ru^{II} in excess of that obtainable by simple partitioning into the film.

As illustrated in Figure 8A electropolymerization occurs from inside the films at the conducting ITO electrode through the film to the outside. The electrochemical and UV−visible results demonstrate increasing growth of poly-$[Ru(vbpy)_3](PF_6)_2$ with the number of reductive scans. The depth-resolved XPS experiments reveal that growth within ITO/SG is uniform past the external surface−solution interface. These results point to rapid growth from inside out through the open porous film structure through spatially isolated channels.

This pattern of growth explains why with partial electropolymerization the electroresponse of the $Os(vbpy)_3^{3+/2+}$ wave in Figure 6A is diffusional. Rather than filling the open film pores from outside in, the pores are selectively filled in parallel across the surface, which leaves diffusion channels open from the external solution to the ITO surface, Figure 8B.

Diffusion also plays a role in the increasingly distorted wave shape for the poly-$[Ru(vbpy)_3]^{3+/2+}$ couple as the extent of polymerization increases. In this case the filling of the diffusional channels presumably inhibits counterion transfer from the external solution into the film, which is required for charge compensation as Ru^{2+} is oxidized to Ru^{3+}.

Film Structure. As expected, the porosity of the sol−gel film can contribute significantly to the success or failure of the electropolymerization procedure. We have found that development of sol−gels with suitable pore and channel sizes is largely a trial and error process. In our experience the conditions described in the Experimental Section were optimal. Variations explored included varying the amount of TX100 added to increase or decrease the film porosity. Less TX100 decreases the number of voids within the gel material and decreases porosity. This limits the diffusion through the film to the ITO surface, which hinders electropolymerization. Adding too much surfactant increases the number and size of the voids to the point that very thin or no gel framework is formed in the gelation process.

The impact of reductive potential scan holds on the porosity of the films toward diffusion is both notable and important. The microscopic origin of the of the effect is not clear, but the effect has a dramatic impact on the ability of the films to act as porous membranes toward diffusion. This response to negative potential scans may also be an important limitation in the use of these films in LED applications where scans to negative potentials or sustained potential holds are required.

Bilayer Effect. Given the evidence for the "vertical" rather than lateral polymer growth from the ITO/SG interface, it is not a surprise that we were unable to prepare structured, electropolymerized "bilayers" with polymerized $[Os(vbpy)_3](PF_6)_2$ confined in layers away from the ITO/SG interface. Rather, the structure suggested by the XPS and electropolymerization results is that rapid growth occurs from the ITO electrode through the membrane to the external solution through intrafilm channels. Partial electropolymerization of $[Ru(vbpy)_3]^{2+}$ followed by $[Os(vbpy)_3]^{2+}$ appears to create a parallel array of channels with separate, parallel networks of Os^{II} and Ru^{II} oxidation and ion migration as shown in Figure 8C.

It was possible to demonstrate a bilayer effect at completely filled films with $[Os(vbpy)_3]^{2+}$ in the external solution. The response of the resulting redox assembly, ITO/SG-poly-$[Ru(vbpy)_3](PF_6)_2$/$[Os(vbpy)_3]^{2+}$ (MeCN), depended on scan rate, but under all conditions could be interpreted with redox events constrained to occur not by diffusion but at the film solution interface.

At the relatively rapid scan rate of 100 mV/s with $[Os(vbpy)_3]^{2+}$ at 3 mM in the external solution, the electrochemical response is that expected for a kinetically inhibited bilayer. On the basis of the voltammograms in Figure 6B,C:

(1) In Figure 6B a positive scan results in a wave of high peak current at $E_{p,a} = 1.1$ V past $E_{1/2} = 0.9$ V for the $Ru^{III/II}$ couple of poly-$[Ru(vbpy)_3](PF_6)_2$. As noted above, the skewing is due to kinetically inhibited counterion migration. This wave arises from oxidation of ITO/SG-poly-$[Ru(vbpy)_3]$-

$(PF_6)_2$ to Ru^{III} followed by Ru^{III} oxidation of Os^{II} at the film−solution interface (eqs 3 and 4). From the differences in $E_{1/2}$ values between the $Ru^{III/II}$ and $Os^{III/II}$ couples, $\Delta G° = -0.45$ eV for interfacial electron transfer between ITO/SG-poly-$[Ru^{III}(vbpy)_3](PF_6)_3$ and $[Os(vbpy)_3]^{2+}$.

$$\text{ITO/SG-poly-}[Ru^{II}(vbpy)_3](PF_6)_2 \xrightarrow[+PF_6^-]{-e^-} \text{ITO/SG-poly-}[Ru^{III}(vbpy)_3](PF_6)_3 \quad E_{1/2} = 0.9\text{V} \quad (3)$$

$$\text{ITO/SG-poly-}[Ru^{III}(vbpy)_3](PF_6)_3| + Os^{II}(vbpy)_3^{2+} \rightarrow \text{ITO/SG-poly-}[Ru^{II}(vbpy)_3](PF_6)_2| + Os^{III}(vbpy)_3^{3+} + PF_6^- \quad \Delta G° = -0.45 \text{ eV} \quad (4)$$

(2) In the reverse scan a small wave is observed for rereduction of Ru^{III} to Ru^{II}, the reverse of eq 3. Further reductive scanning results in rereduction of Os^{III} to Os^{II} but at a more negative potential, $E_{p,c} \sim 0.2$ V, compared to Figure 6A, and the wave is skewed to the negative potential side. These observations are consistent with slow Os^{III} rereduction by Ru^{II} at the film−solution interface, which is expected since the reaction is nonspontaneous by ~0.45 eV with the interfacial electron-transfer mechanism shown in eqs 5 and 6.

$$\text{ITO/SG-poly-}[Ru^{II}(vbpy)_3](PF_6)_3| + Os^{III}(vbpy)_3^{3+} \rightarrow \text{ITO/SG-poly-}[Ru^{III}(vbpy)_3](PF_6)_2| + Os^{II}(vbpy)_3^{2+} + PF_6^- \quad \Delta G° = +0.45 \text{ eV} \quad (5)$$

$$\text{ITO/SG-poly-}[Ru^{III}(vbpy)_3](PF_6)_3 \xrightarrow[+PF_6^-]{+e^-} \text{ITO/SG-poly-}[Ru^{II}(vbpy)_3](PF_6)_3 \quad E_{1/2} = 0.9\text{ V} \quad (6)$$

(3) In Figure 6C at the slow scan rate of 5 mV/s, the form of the voltammetric response becomes that of voltammetric current−time experiment. In this case induced oxidation of Os^{II} to Os^{III} in the external solution occurs near the potential for the $Ru^{III/II}$ couple at $E_{1/2} = 0.95$ V consistent with counterion diffusion no longer being rate limiting. In this case the scan rate is sufficiently slow that the majority of Os^{III} rereduction also occurs at or near $E_{1/2}$ for the $Ru^{III/II}$ couple. Reduction of Os^{III} near 0.9 V however is not complete during the scan and an additional wave with a relatively smaller peak current appears at or near $E_{1/2} = 0.45$ V for the $Os^{III/II}$ couple.

Photophysical Properties. The photophysical properties of the ITO/SG-poly-$[Ru(vbpy)_3](PF_6)_2$ composites were of interest for comparison with the excited-state properties of closely related Ru−bpy chromophores in other nonisotropic environments such as on metal oxide surfaces,[40−43] in organic thin films, such as polymethylmetacrylate (PMMA),[44−46] and, in particular, in electropolymerized thin films of poly-[Ru$(vbpy)_3](PF_6)_2$ on conducting substrates.[36,47] We also have a long-term interest in combining the electron-transfer properties of the composite films with the excited-state properties of the complexes in electroluminescent and chemiluminescent applications.[22,48]

The photophysical properties of the Ru^{II*} MLCT chromophore in ITO/SG-poly-$[Ru(vbpy)_3](PF_6)_2$ are, as expected, more complex than those of related complexes, e.g., Ru$(dmb)_3^{2+}$, in solution.

Emission from both ITO/SG-poly-$[Ru(vbpy)_3](PF_6)_2$ and ITO/poly-$[Ru(vbpy)_3](PF_6)_2$ is red-shifted and broadened, Figure 5A. For the latter this has been attributed to the presence of low-energy trap sites in the highly cross-linked network of ruthenium complexes.[36] Excitation and intrafilm energy transfer result in population of these states, which have shortened lifetimes because of their low energy gaps.

The enhanced quantum yield of ~10 and blue-shifted emission for ITO/SG-poly-$[Ru(vbpy)_3](PF_6)_2$ compared to the same electropolymerized chromophore on ITO is notable in this regard. As implied by the diagram in Figure 8, electropolymerization in the channels of the sol−gel restricts the extent of electropolymerization. This leaves both unreacted vinyl groups and a low (1−2) dimensional polymeric network in contrast with the high (2−3) dimensional network in polymeric films on ITO. This internal control of structure by the pore voids may decrease the number of low-energy trap sites and the extent of communication throughout the films by energy-transfer migration.

These effects also appear in the lifetime data in Figure 5B and Table 1. In solution, the lifetime of the model Ru$(dmb)_3^{2+*}$ is 950 ns in deaerated CH_3CN[49] and the decay is exponential. The decay kinetics both in the electropolymerized films on ITO and in the sol−gel are highly nonexponential. The excited states are sensitive to environment, and nonexponentiality arises from the heterogeneity of environments in the films and the existence of dynamical intrastrand energy transfer and quenching at low-energy trap sites.[50]

A comparison among the three sets of data is revealing. The greatly decreased lifetime in ITO/poly-$[Ru(vbpy)_3](PF_6)_2$ compared to the solution model complex has been explained by intrafilm energy transfer and trap site quenching as described above. As is clear from the fitting parameters and by the inspection of the data in Figure 5B, there are clearly time domains of different decay behavior in ITO/SG-poly-$[Ru(vbpy)_3](PF_6)_2$. Over the first ~200 ns the decay is

(40) Trammell, S. A.; Yang, P.; Sykora, M.; Fleming, C. N.; Odobel, F.; Meyer, T. J. *J. Phys. Chem. B* **2001**, *105*, 8895−8904.
(41) Meyer, T. J.; Meyer, G. J.; Pfennig, B. W.; Schoonover, J. R.; Timpson, C. J.; Wall, J. F.; Kobusch, C.; Chen, X. H.; Peek, B. M.; Wall, C. G.; Ou, W.; Erickson, B. W.; Bignozzi, C. A. *Inorg. Chem.* **1994**, *33*, 3952−3964.
(42) Striplin, D. R.; Wall, C. G.; Erickson, B. W.; Meyer, T. J. *J. Phys. Chem. B* **1998**, *102*, 2383−2390.
(43) Pfennig, B. W.; Chen, P. Y.; Meyer, T. J. *Inorg. Chem.* **1996**, *35*, 2898−2901.
(44) Dattelbaum, D. M.; Meyer, T. J. *J. Phys. Chem. A* **2002**, *106*, 4519−4524.
(45) Adelt, M.; Devenney, M.; Meyer, T. J.; Thompson, D. W.; Treadway, J. A. *Inorg. Chem.* **1998**, *37*, 2616.
(46) Fleming, C. N.; Jang, P.; Meyer, T. J.; Papanikolas, J. M. *J. Phys. Chem. B* **2004**, *108*, 2205−2209.
(47) Kajita, T.; Leasure, R. M.; Devenney, M.; Friesen, D.; Meyer, T. J. *Inorg. Chem.* **1998**, *37*, 4782−4794.
(48) Maness, K. M.; Terrill, R. H.; Meyer, T. J.; Murray, R. W.; Wightman, R. M. *J. Am. Chem. Soc.* **1996**, *118*, 10609−10616.
(49) Strouse, G. F.; Schoonover, J. R.; Duesing, R.; Boyde, S.; Jones, W. E.; Meyer, T. J. *Inorg. Chem.* **1995**, *34*, 473−487.
(50) Chen, P.; Meyer, T. J. *Chem. Rev.* **1998**, *98*, 1439−1477.

dominated by fast decay processes with $\tau_2 = 243$ ns. Past ~200 ns, decay in the sol−gel slows considerably and is dominated by a slow decay component with $\tau_3 = 1074$ ns. These observations point to the existence of trap sites in the film, to which only a fraction of the excited states have access by intrastrand energy transfer. The longer lived components are presumably associated with intrinsic, unquenched sites, which contribute to the blue side of the emission manifold and have extended lifetimes because of the rigid medium effect[50,51] and the resulting enhanced energy gap.

Acknowledgment is made for support of this research to the Department of Energy and the Los Alamos National Laboratory. We also thank Xingu Wen of UNC Chapel Hill for performing the XPS analysis of the composite films depth profiles.

IC048623R

(51) Chen, P.; Meyer, T. J. *Inorg. Chem.* **1996**, *35*, 5520−5524.